(Pyridyl)benzoazole ruthenium(III) complexes: kinetics of ligand substitution reaction and potential cytotoxic properties

Reinner Ochola Omondi, [1] Deogratius Jaganyi*[2] Stephen Otieno Ojwach, [1] Amos Akintayo Fatokun[3]

[1]School of Chemistry and Physics, University of KwaZulu-Natal, Private Bag X01, Scottsville, Pietermaritzburg, 3209, South Africa

[2]School of Science, College of Science and Technology, University of Rwanda, P.O. Box 4285, Kigali, Rwanda

[3]School of Pharmacy and Biomolecular Sciences, Faculty of Science, Liverpool John Moores University, Liverpool L3 3AF, UK

*Deogratius Jaganyi:deojaganyi@gmail.com

Highlights

- Ruthenium(III) complexes were successfully synthesised.

- The substitution of the coordinated chloro ligands happened simultaneously.

- Density functional theoretical calculations supports substitution kinetic results.

- Complexes demonstrate low antineoplastic properties against Hela cancer cells.

- Molecular docking of the compounds demonstrate good affinity for DNA molecule.

Graphical abstract
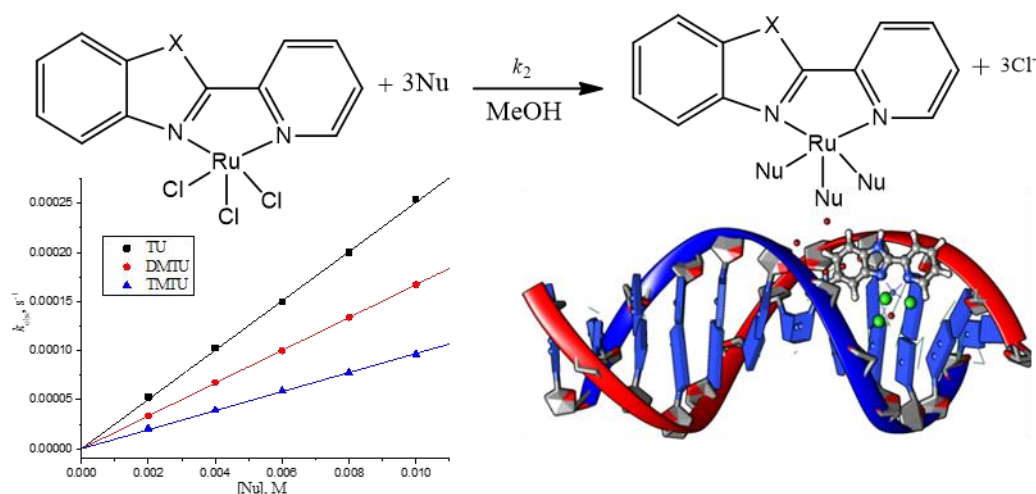
In all substitution kinetics reactions, a single step, considered to be the displacement of the coordinated chlorides was seen with no solvation pathway. Due to the symmetrical nature of the investigated ruthenium(III) complexes, the three chloride ligands are equally substituted simultaneously. The docking experiments reveal that the binding energies of the complexes have direct correlation to their kinetic stability.

Keywords: ruthenium(III) complexes; substitution kinetics; density functional theory; molecular docking; cytotoxicity; anti-cancer activities

Abstract

The present work investigates the kinetics of ligand substitution reaction and anticancer activities of the complexes, [{2-(2-pyridyl) benzimidazole} RuCl$_3$] (**C1**), [{2-(2-pyridyl) benzoxazole} RuCl$_3$] (**C2**), [{2-(2-pyridyl) benzothiazole} RuCl$_3$] (**C3**) and [{1-propyl-2-(pyridin-2-yl)-H-benzoimidazole} RuCl$_3$] (**C4**). The substitution kinetics reaction of the complexes with the three bio-relevant nucleophiles, *viz.*: thiourea (**TU**), 1, 3-dimethyl-2-thiourea (**DMTU**) and 1, 1, 3, 3-tetramethyl-2-thiourea (**TMTU**) was investigated under

pseudo first-order conditions as a function of concentration and temperature using UV-Visible spectrophotometer. The substitution of the coordinated chloride was controlled by the electronic effect. The order of reactivity of the complexes with the nucleophiles is in the form **C1** > **C2** > **C3** > **C4** which is in line with the density functional theory (DFT) studies. The complexes showed minimal anticancer activity against the HeLa cell line, which is in contrast to the molecular docking experiments that exhibited stronger DNA binding affinities.

Introduction

The documented clinical limitations of *cisplatin* and its second and third generation analogues have triggered the search for other anticancer agents containing metals other than platinum. Metals such as iridium, gold, cobalt, ruthenium and silver have so far shown good cytotoxicity [1-4]. These complexes appear to possess markedly lower toxicities, high tumour selectivity and enhanced solubility. Among the non-platinum metal compounds, ruthenium complexes seem to be the most promising class due to their structural and coordination properties. These properties have been considered in a number of excellent reviews [5-8] and they include (i) accessibility to multiple oxidation states at physiological conditions, which makes them suitable for pharmaceutical use; (ii) octahedral geometry which differs from the square-planar molecular geometry of platinum(II) compounds, this allows for tuning of the steric and electronic properties of the complexes; (iii) a rate of ligand substitution kinetics that is close to those of cellular processes, giving the drug high kinetic stability and hence reducing side reactions; (iv) the ability of ruthenium metal to mimic iron in binding to serum transferrin and albumin proteins, which transports and solubilises iron in cytoplasm and thereby exploiting the body's mechanism of nontoxic delivery of iron.

Over the years, most research groups have evaluated ruthenium complexes for their potential to inhibit the growth of tumours. The key focus has been on the interaction between active ruthenium compounds and their possible targets such as RNA and DNA [9-10]. It is widely accepted that the antineoplastic properties of ruthenium(II) and ruthenium(III) compounds is directly related to their ability to bind to DNA [11], although a few exceptions have been also reported [12]. Contributing to this field of study, Sadler [13-14] and Dayson [15-16] have developed structure-activity relationship using monofunctional compounds [Ru(η6-C_6H_6)(en)(Cl)]$^+$. The general mechanism for these half-sandwich ruthenium(II) arene complexes encompasses rapid loss of the choro ligand with the formation of more reactive aqua species, followed by the substitution kinetics of the labile aqua ligand by DNA and RNA.

In the recent years, Bugarčić and his co-workers [17-21] have examined the anticancer activities of a series mononuclear ruthenium(II) chlorophenyl terpyridine complexes and establishing their rate of substitution kinetics using L-histidine (L-His) and guanine derivatives (i.e., 9-methylguanine (9MeG) and 5′-GMP). They found that the rates of substitution kinetics of these complexes strongly depend on the nature of the inert chelating ligand on their inductive effect and the steric hindrance including the charge of the entering nucleophile.

Two ruthenium(III) complexes, KP1019 and NAMI-A, are presently among the most successful drug candidates to enter human clinical trials [22-23]. The preliminary investigations of the two ruthenium compounds demonstrate that they might be promising in the treatment of drug-resistant tumours, as they are effective against cancerous cell lines that are highly resistant to other anticancer agents such as cisplatin and doxorubicin. Despite, the success of these two ruthenium compounds, their mode of mechanism remains a matter of debate. The *in vitro* cytotoxic properties of a series of ruthenium(III) complexes with

dithiocarbamato ligands towards a panel of human tumour cell lines have been investigated [24-26]. The biological assays of most of these complexes on human tumour cell lines point out intriguing selectivity and antiproliferative properties.

Building on the existing knowledge we have investigated the reactivity of mononuclear ruthenium(III) complexes by varying the identity of the heteroatoms on the inert ligand architecture. We have also examined their antineoplastic properties. Hence in this contribution we report the substitution kinetics and anticancer activities of ruthenium(III) complexes supported by 2-(2-pyridyl)benzoazole ligands with thiourea nucleophiles *viz*; TU, DMTU, TMTU. Thiourea nucleophiles act as good model compounds for thioether and thiolate which are present in the cytoplasm. The binding of metal complexes with S-containing biomolecules is accountable for the occurrence of toxic effects. The structures of the complexes and nucleophiles used in this study are shown in Scheme 1 and 2, respectively. The experimental work is supported by computational density functional theory (DFT) studies.
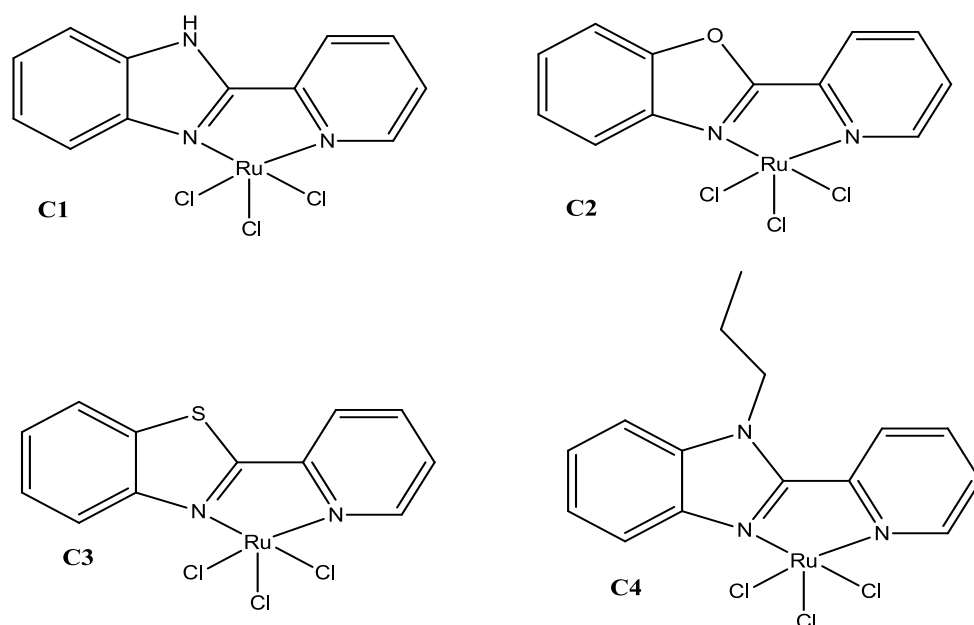
Scheme 1: Structures of the investigated mononuclear (pyridyl)benzoazole ruthenium(III) complexes.
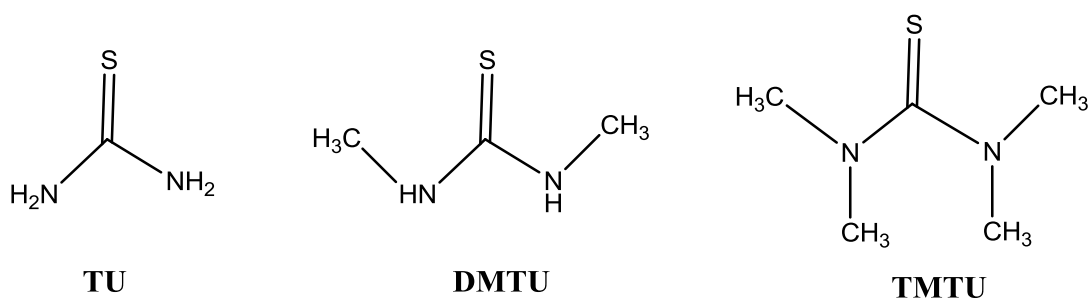
Scheme 2: Structures of the examined thiourea nucleophiles and its derivatives

Experimental

Chemicals

All synthetic procedures were carried out under a nitrogen atmosphere using standard Schlenk techniques. Ruthenium(III) chloride hydrate ($RuCl_3.xH_2O$, 99.98%) was purchased from Merck and used as supplied. Methanol was obtained from Merck and distilled over magnesium prior to use. Sodium perchlorate monohydrate ($NaClO_4.H_2O$, 98%), lithium chloride (LiCl, 99%), thiourea (TU, 99%), N,N-dimethyl-2-thiourea (DMTU, 99%), N,N,N,N-tetramethyl-2-thiourea (TMTU, 98%) were all obtained from Sigma-Aldrich and used as supplied.

Characterisations and instrumentations

Thermal Scientific Flash 2000 and a Carlo Erba Elemental Analyzer 1106. Mass spectrometry measurements were recorded on an LC Premier micro-mass spectrometer. Kinetic experiments were performed on Varian Cary 100 Bio UV-Visible spectrophotometer with an attached Varian Peltier temperature-controller and an online kinetic applications and the temperature of the instrument was controlled within ± 0.1 °C.

Preparation of (pyridyl)benzoazole ligands

The following ligands, namely, 2-(2-pyridyl)benzimidazole (**L1**), 2-(2-pyridyl)bezoxazole (**L2**), 2-(2-pyridyl)bezothiazole (**L3**) and 1-propyl-2-(pyridin-2-yl)-1H-benzo[d]imidazole (**L4**) were synthesised for this investigation. The ligands, **L1**-**L3** were all synthesised using a method previously described in literature [27]. For the preparation of **L4**, this method was slightly modified as described by Ogweno *et al* [28].

Synthesis of (pyridyl)benzoazole ruthenium(III) complexes

Synthesis of [{2-(2-pyridyl) benzimidazole}RuCl₃] (C1)

Complex **C1** was synthesised according to our published literature procedure [28]. A mixture of ligand **L1** (0.09 g, 0.48 mmol) and RuCl₃.3H₂O (0.10 g, 0.48 mmol) was refluxed in absolute ethanol (20 mL) for 4 h. A brown precipitate was collected by filtration, washed thoroughly with excess ethanol and dried to obtain complex **C1** as a brown solid. Yield = 0.08 g (38%). TOF MS-ES, m/z (%) 402.07, (M^+ + H). Anal. Calcd (%) for $C_{12}H_9Cl_3N_3Ru$: C, 35.80; H, 2.25; N, 10.44. Found (%): C, 35.98; H, 2.19; N, 10.66.

Synthesis of [{2-(2-pyridyl)benzoxazole}RuCl₃] (C2)

Complex **C2** was prepared following the synthetic procedure for **C1**, using ligand **L2** (0.21 g, 0.98 mmol) and RuCl₃·3H₂O (0.20 g, 0.98 mmol) to afford a brown solid. Yield = 0.395 g (31%). TOF MS-ES, m/z (%) 404.12, (M^+ + H). Calcd (%) for $C_{12}H_8Cl_3N_2ORu$: C, 35.71; H, 2.00; N, 6.94; O, 3.96. Found (%): C, 35.41; H, 1.78; N, 7.03; O, 4.06.

Synthesis of [{2-(2-pyridyl)benzothiazole}RuCl₃] (C3)

The procedure used in the synthesis of complex **C1** was used in the preparation of **C3**, using ligand **L3** (0.21 g, 0.98 mmol) and RuCl₃·3H₂O (0.20 g, 0.98 mmol) to yield a light brown

solid. Yield = 0.411g (76%). TOF MS-ES, m/z (%) 420.09 (M$^+$ + H). Calcd (%) for C$_{12}$H$_8$Cl$_3$N$_2$RuS: C, 34.34; H, 1.92; N, 6.67; S, 7.64. Found (%): C, 34.63; H, 1.02; N, 6.92; S, 7.47.

*Synthesis of [{1-propyl-2-(pyridin-2-yl)-H-benzoimidazole}RuCl$_3$] (**C4**)*

This complex was synthesised following the synthetic procedure described for complex **C1**, using ligand **L4** (0.21 g, 0.98 mmol) and RuCl$_3$·3H$_2$O (0.20 g, 0.98 mmol) to produce complex **C4** as a brown solid. Yield = 0.09 g (43%). TOF MS-ES, m/z (%) 408, (M$^+$ + -Cl). Calcd (%) for C$_{15}$H$_{15}$Cl$_3$N$_3$Ru: C, 40.51; H, 3.40; N, 9.45. Found (%): C, 40.09; H, 3.08; N, 9.64.

Preparation of nucleophile solutions for kinetic measurements

The stock solutions of nucleophiles, *viz.* thiourea (TU), 1,3-dimethyl-2-thiourea (DMTU) and 1,1,3,3-tetramethyl-2-thiourea (TMTU) were prepared shortly before use by dissolving known amounts of the nucleophiles in 0.1 M (adjusted with NaClO$_4$ and LiCl) methanol solutions to afford a concentration of approximately 150 times greater than that of the metal complex. The other nucleophile solutions were prepared by subsequent dilutions of the same stock solutions to obtain a series of standards of 120, 90, 60 and 30 times the concentration of the metal complex. The NaClO$_4$ was used because perchlorate ions do not bind to the ruthenium(III) metal centre. In addition, LiCl was added to prevent possibility of any spontaneous solvolytic reactions.

Kinetic procedure

The rate of substitution of the coordinated chloride from each of the four compounds of ruthenium(III) was investigated using a series of neutral sulphur-donor nucleophiles *viz.* TU, DMTU and TMTU using UV-Vis spectrophotometer. All kinetic investigations were

conducted under pseudo-first order conditions, in which the concentration of the incoming nucleophile was at least 30-fold excess of the complexes so as to force the substitution reactions to completion [29]. The working wavelengths were pre-determined by recording spectra of the reaction mixture over the wavelength range 200–850 nm to establish suitable wavelengths at which their kinetic measurements could be investigated.

Computational modelling

Computational modelling was performed by the Gaussian09 program package to gain a clear understanding of the electronic and structural differences of the investigated compounds [30]. The geometry optimisations, frequency calculations, and mapped molecular orbital diagrams were carried out at density functional theoretical (DFT) level based on B3LYP/LanL2DZ (Los Alamos National Laboratory 2 double ξ) level theory [31-32]. The singlet state was adopted due to the low electronic spin of (pyridyl)benzoazoles ruthenium(III) compounds. The compounds were computed with methanol solvent, considering the solvolysis effects by means of the Conductor Polarizable Continuum Model [33-34].

Cytotoxicity assay

The human cervical carcinoma HeLa cells were used for the cytotoxicity experiments as previously reported [35]. They were grown in 75 cm^2 tissue culture flasks using Dulbecco's Modified Eagle Medium (DMEM) supplemented with 10% Foetal Calf Serum, 2 mM L-glutamine, 1% non-essential amino acid and 1% antibiotic-antimycotic solution. They were incubated at 37 °C in a humidified atmosphere of 5% CO_2. At about 80-90% confluency, the medium was removed and cultures were rinsed with pre-warmed PBS, trypsinised and seeded into micro-clear, flat-bottom 96-well plates at a density of 5 x 10^4 cells per ml (100 µl/well). After 24 h, a range of concentrations up to 400 µM was prepared from the DMSO stock

concentration of each tested compound and added to the cultures, each in triplicate (the final highest concentration (v/v) of DMSO in the growth medium that the cultures were exposed to was confirmed not to affect cell viability), and plates were incubated for 48 h, after which viability was assessed using the 3-(4,5-Dimethyl-2-thiazolyl)-2,5-diphenyl-2H-tetrazolium bromide [MTT] assay [36]. This was done by adding to each well 10 µl of the MTT solution (5 mg/ml, prepared in sterile PBS) before incubating the plates for 3 h. Thereafter the content of each well was aspirated and 100 µl of DMSO was added to dissolve the insoluble formazan. The absorbance of each well was then read at a wavelength of 570 nm using the CLARIOstar plate reader (BMG Labtech). Changes to the morphology of the cells caused by the treatments were monitored on an Olympus CKX41 microscope fitted with an Olympus DP71 U-TVIX-2 camera. Images were captured using the Olympus cellSens entry software.

For each treatment the mean of the triplicate values was calculated. The mean of the control cultures (cultures not exposed to treatment with any compound) was then set to 100% and the mean viability for each concentration normalised to it. Values are represented as Mean ± SEM (standard error of the mean). Statistical analyses were done using GraphPad (Version 7.03, GraphPad Software, Inc., CA, USA). Statistically significant differences between the means were determined using analysis of variance (ANOVA) followed by a post-hoc test for multiple comparisons (Tukey test). A P-value of less than 0.05 was considered statistically significant. IC_{50} for each compound was determined using GraphPad by fitting the data to the non-linear regression of log [inhibitor] versus response (3 parameters or 4 parameters (variable slope)).

Molecular docking experiment
Molecular docking studies were performed using HEX 8.0.0 software, which uses spherical polar Fourier correlations to accelerate the calculations. All calculations were carried out on an

Intel Core i3-4170 CPU using the following parameters; correlation type: (shape + electro); search order: 25; receptor/ligand: 180; step sizes: 7.5; grid dimension: 0.6; number of solutions: 2000. The structures of the compounds were sketched by CHEMSKETCH [37] and converted to PDB format from MOL format using Mercury software [38]. The crystal structure of the B-DNA dodecamer d(CGCGAATTCGCG)2 (PDB ID: 1BNA) was downloaded from the protein data bank [39]. All water molecules were removed before docking calculations with the examined compounds. The docked poses were visualised using UCSF Chimera software [40].

Results

Kinetic analyses

All substitution kinetics experiments showed that all reactions were characterised by a single step that could be studied using UV-Visible spectroscopy. A typical Spectral changes and kinetic trace obtained by monitoring the reaction between TU and C3 as shown in Figure 1.
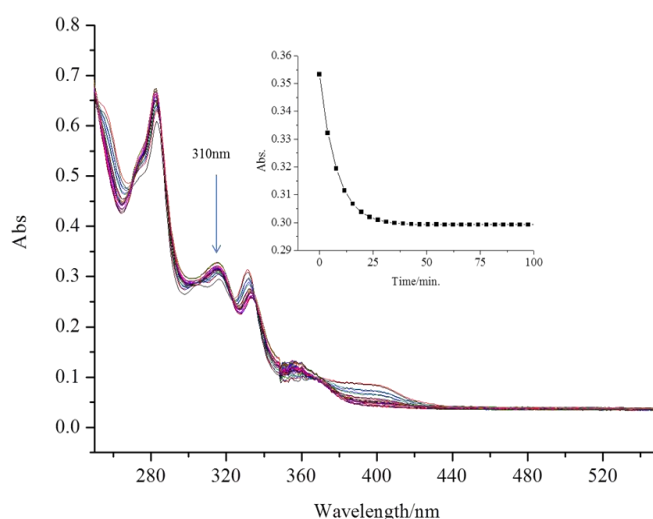
Figure 1: Spectral changes and kinetic trace obtained from the UV-Visible spectrometer with a single exponential fit for the reaction between **C3** (5.0×10^{-4} mol dm^{-3}) and TU (1.5×10^{-2}

11

mol dm^{-3}) in methanol followed at 310 nm, $I = 0.1$ M (0.01 M LiCl, 0.09 M NaClO$_4$), T = 298 K.

All the kinetic traces for the substitution reactions provided excellent fits to first-order exponential decay to produce, *pseudo*-first-order rate constants, k_{obs}, at specific concentrations of the nucleophiles and temperature. The k_{obs}, were established by a nonlinear least square fit of the absorbance-time data to Equation 3.1 using Origin 7.5® software graphical analysis software [41].

$$A_t = A_o + (A_o - A_\infty)\, e^{(-k_{obs.})t} \tag{1}$$

where A_o, A_t and A_∞ represent absorbance of the mixture of the reaction at the start of the reaction at time, t and at the end of the reaction, respectively. The dependence of the rate constant on the concentration of the incoming nucleophiles was analysed for all the examined nucleophiles while keeping the temperature at 25 °C. The k_{obs} was calculated as a mean of at least three independent kinetic experiments. The second-order rate constant, k_2, for the reactions of the ruthenium(III) complexes with the incoming nucleophiles were attained from the slopes of the graphs of k_{obs} versus the concentration of the incoming nucleophile using Origin 7.5® software. Representative plots for complex **C1** are shown in Figure 2. In all cases, the reactions displayed a first-order dependence on the concentration of the incoming nucleophile.
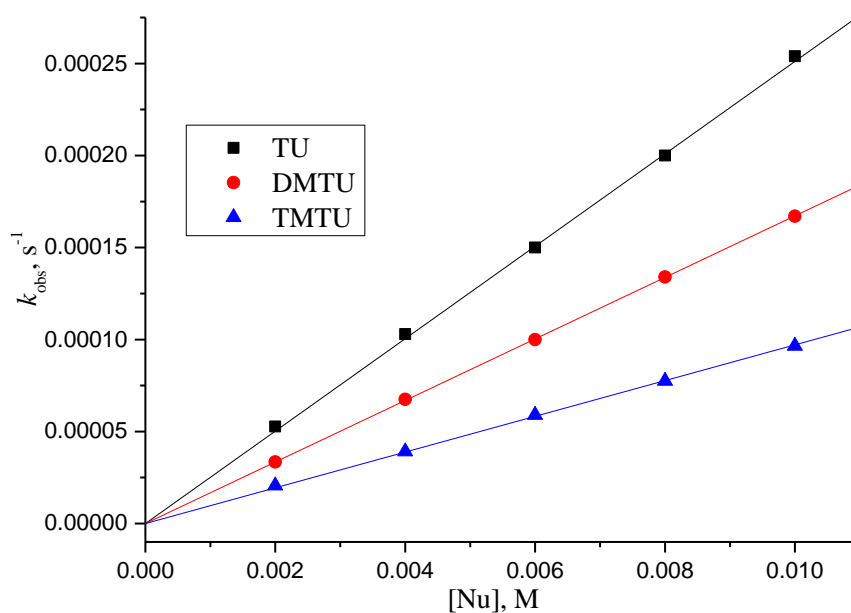
Figure 2: Concentration dependence of k_{obs} for the substitution of chlorides from **C1** (1.0×10^{-4} M) by thiourea nucleophiles in methanol solution, $I = 0.1$M (0.01 M LiCl, 0.09 M NaClO$_4$) at 298 K.
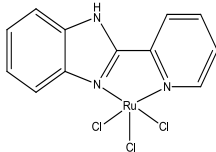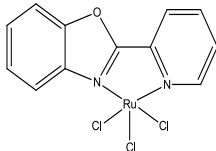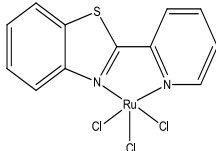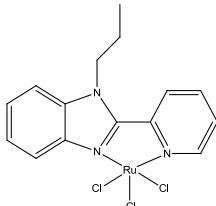
The plots gave straight line fits with zero intercept for each of the investigated nucleophiles. Therefore, the proposed mechanism of substitution is as shown in Scheme 3 and the corresponding rate law is represented by Equation 1, showing that the kinetic pathway is irreversible and does not depend on the solvent. The values of the second-order rate constant k_2, which were obtained from the slopes of these plots at 25 °C are summarised in Table 1.

Nu = TU, DMTU, TMTU

X = NH (**C1**)
O (**C2**)
S (**C3**)
N-propyl (**C4**)
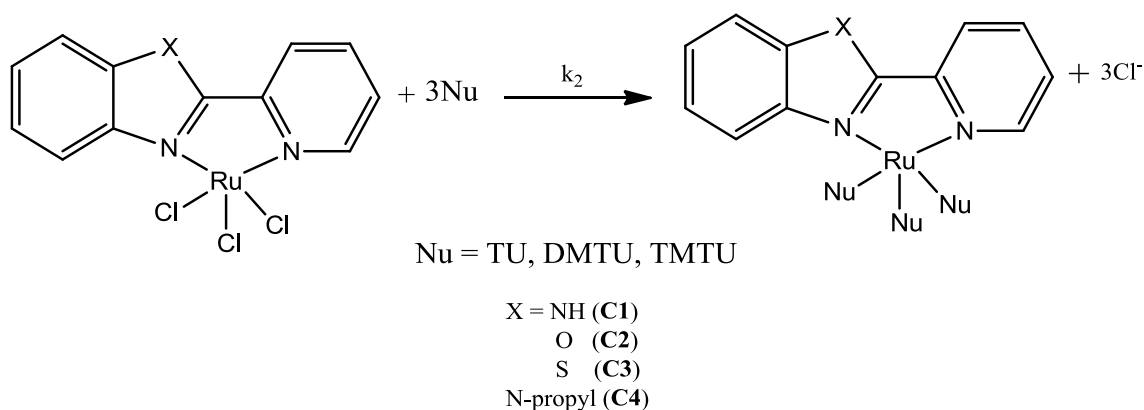
Scheme 3: Proposed substitution mechanism for the ruthenium complexes supported by 2-(2-pyridyl)benzoazole ligands

$$k_{obs} = k_2 \text{ [nucleophile]} \qquad (1)$$

Table 1: Summary of the rate constants and activation parameters for the substitution of chloride by TU, DMTU and TMTU in methanol solution, $I = 0.1$ M (0.01 M LiCl, 0.09 M NaClO$_4$) at 298 K

Complex	Nu	k_2/M^{-1}s^{-1}	$\Delta H^{\neq}$/kJmol^{-1}	$\Delta S^{\neq}$/Jmol^{-1}K^{-1}
C1	TU	$(2.47 \pm 0.02) \times 10^{-2}$	65 ± 1	-43 ± 3
	DMTU	$(1.67 \pm 0.03) \times 10^{-2}$	76 ± 1	-11 ± 4
	TMTU	$(9.7 \pm 0.05) \times 10^{-3}$	78 ± 1	-20 ± 3
C2	TU	$(1.33 \pm 0.04) \times 10^{-2}$	68 ± 1	-48 ± 3
	DMTU	$(9.0 \pm 0.02) \times 10^{-4}$	83 ± 2	-25 ± 5
	TMTU	$(7.0 \pm 0.03) \times 10^{-4}$	84 ± 1	-24 ± 3
C3	TU	$(4.6 \pm 0.02) \times 10^{-3}$	64 ± 1	-60 ± 3
	DMTU	$(5.0 \pm 0.02) \times 10^{-4}$	84 ± 2	-27 ± 6
	TMTU	$(2.0 \pm 0.01) \times 10^{-4}$	85 ± 1	-37 ± 4
C4	TU	$(2.0 \pm 0.01) \times 10^{-3}$	69 ± 1	-74 ± 3
	DMTU	$(4.0 \pm 0.01) \times 10^{-4}$	88 ± 1	-13 ± 3
	TMTU	$(1.0 \pm 0.01) \times 10^{-4}$	90 ± 1	-19 ± 3

The second order rate constant k_2, was also determined as a function of temperature, over a temperature range of 25-45 °C at intervals of 5 °C to obtain the activation parameters for substitution of the coordinated chlorides from ruthenium(III) complexes. The enthalpy of activation ($\Delta H^{\neq}$) and entropy of activation ($\Delta S^{\neq}$), were calculated using Eyring equation [42]. The values of $\Delta S^{\neq}$ and $\Delta H^{\neq}$ were calculated from the intercepts and slopes of Eyring plots,

respectively. These parameters are tabulated in Table 1. Representative Eyring plots obtained

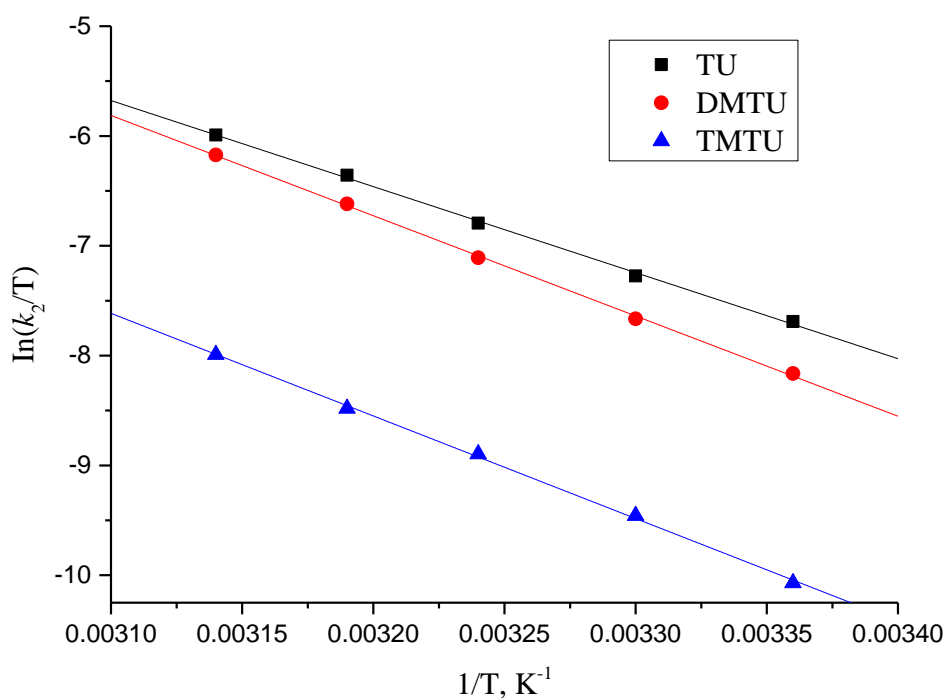for the reactions of **C1** with the three nucleophiles are shown in Figure 3.

Figure 3: Eyring plot obtained for the substitution of chloride from **C1**, by thiourea

nucleophiles $I = 0.1$ M (0.01 M LiCl, 0.09 M NaClO$_4$) in methanol at various temperatures in

the range 25 - 45 °C.

Computational calculations

Computational analyses of the ruthenium(III) complexes were determined in order to help

explain the kinetic trends observed and the influence of the molecular structures as well as the

electronic properties of the complexes on the observed reactivity. Table 2 shows an extract of

the geometry optimised structures, LUMO and HOMO frontier molecular orbitals for the

complexes while Table 3 shows a summary of the corresponding properties of the frontier

molecular orbitals: HOMO-LUMO, NBO atomic charges and bond lengths.

Table 2: DFT frontier molecular orbitals and minimum energy structures of ruthenium(III) complexes **C1**-**C4** as established by density functional theory using B3LYP level of theory and LANL2DZ basis set
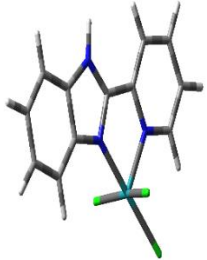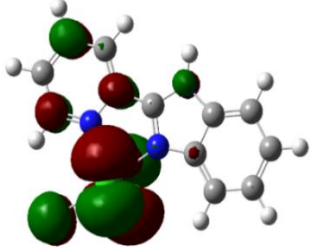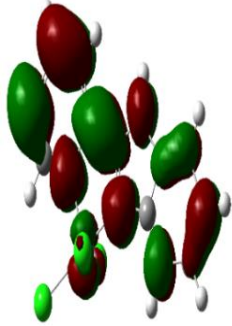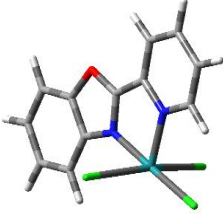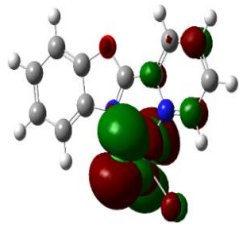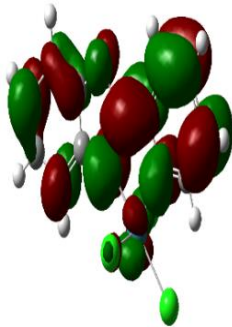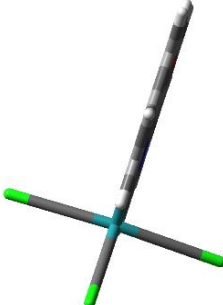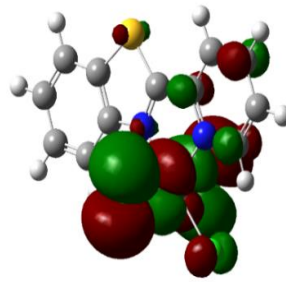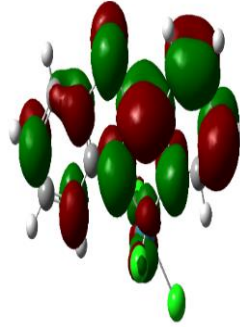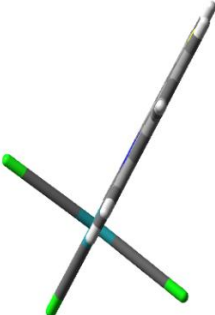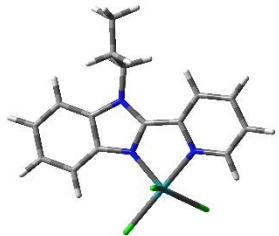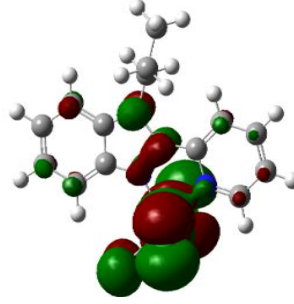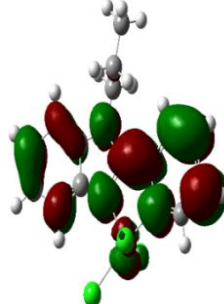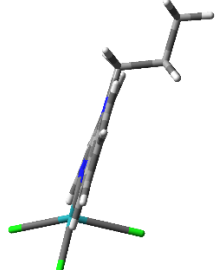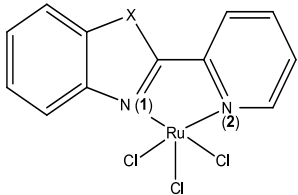
Geometry-optimised structure	HOMO map	LUMO map	Planarity
C1			
C2			
C3			
C4			

Table 3: Summary of the data obtained from the DFT calculations for the ruthenium(III) complexes

X= NH (**C1**); O (**C2**); S (**C3**); N-propyl (**C4**)

	C1	C2	C3	C4
LUMO /eV	-3.67	-3.82	-3.80	-2.90
HOMO /eV	-6.79	-6.96	-6.97	-6.74
ΔE /eV	3.12	3.14	3.16	3.83
Chemical hardness (η)	3.12	3.14	3.16	3.83
Electronic chemical potential (μ)	-5.23	-5.39	-5.39	-4.82
Electrophilicity index (ω)	4.38	4.63	4.60	3.03
NBO Charges				
Ru	0.354	0.348	0.344	0.316
X	-0.394	-0.251	0.358	-0.170
N_1	-0.382	-0.347	-0.313	-0.310
Bond Length (Å)				
Ru-Cl bond length [a]	2.43	2.42	2.40	2.38
Ru-N_1	2.06	2.07	2.11	2.30

NBO = natural bond orbital, [a]average Ru-Cl bond length of three chlorides.

In vitro cytotoxicity testing to assess potential anti-cancer activity

All the complexes were screened for their *in vitro* cytotoxicity against the HeLa cell, with doxorubicin used as a standard reference. The effects of doxorubicin (up to 20 µM) and the complexes (each up to 400 µM) on cell viability were determined after cells were exposed to them for 48 h. Doxorubicin decreased HeLa cell viability in a concentration-dependent manner, with an IC_{50} of 0.8 ± 0.2 µM, while the complexes did not cause significant reductions in cell viability at the concentrations tested, except that **C2** at 400 µM reduced viability to $82.6 \pm 0.3\%$ (P<0.05) (Table 4).

Table 4: *In vitro* cytotoxic activity results (IC$_{50}$ µM) of ligands and complexes against Hela cell[a]

Compound	IC$_{50}$ (in µM)
Doxorubicin[b]	0.8
C1	>200
C2	>200
C3	>200
C4	>200
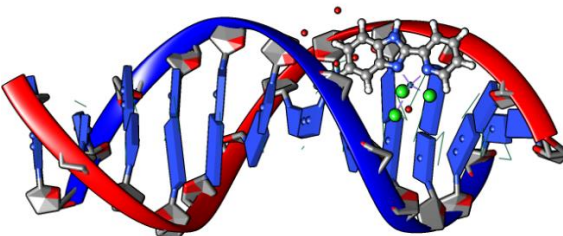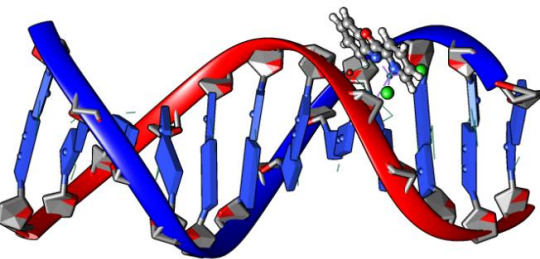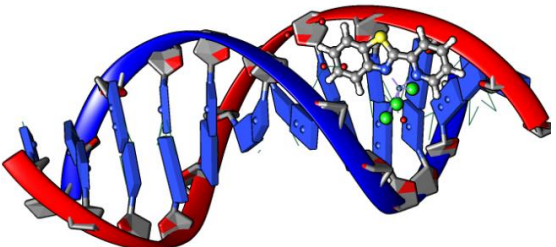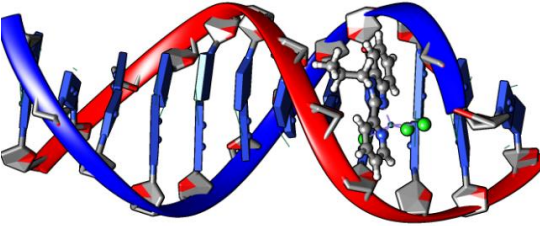
[a]IC$_{50}$ values obtained by MTT assay results after 48 h drug exposure at various concentrations.

Results are presented as mean ± SD of three independent experiments. [b]Reference drug.

Molecular docking analyses

The investigated compounds were docked within the DNA duplex of sequence d(CGCGAATTCGCG)$_2$ dodecamer (PDB ID: 1 BNA) to determine the binding site inside the DNA. Docked images and relative binding energies of the ruthenium(III) complexes are summarised in Table 4.

Table 5: Molecular docking results of ruthenium(III) complexes

Complex	Docked images of complexes	Relative binding energy of complexes (kJ/Mol)
C1		-216.57
C2		-220.63
C3		-226.14
C4		-244.03

Discussion

Comparing the rates of displacement of the coordinated chloride from the ruthenium(III) complexes, a clear general trend is observed from the reactivity data in Table 1. Using the rate constant of **C1** with TU as a reference point, the ratio of the rate of substitution of the chloro from the complexes is 10:5:2: 1 for **C1**: **C2**: **C3**: **C4**, respectively. Therefore, the reactivity for the substitution of the chloride ligands by the thiourea nucleophiles decreases in the order of

C1 > C2 > C3 > C4. A similar order of reactivity trend was observed for all the investigated nucleophiles. The difference in reactivity is ascribed to the electronic effects of the heteroatoms of benzoazole of the ligand architecture.

The identity of the heteroatom NH (**C**1); O (**C2**); S (**C3**); and N-propyl (**C4**) on the inert ligand framework affects the rate of substitution of the coordinated chlorides from ruthenium(III) complexes. The electronegativity of the heteroatoms aids in the withdrawal of electron density from the ligand, enhancing π-back bonding and thereby creating a more electrophilic metal centre [43]. Thus increasing the rate of the substitution kinetic reaction. Evidence of π-back bonding is shown by the magnitude of the negative charge on the nitrogen atom attached to the ruthenium(III) metal centre. There is an increase of the negative NBO charge of the N_1 with increase in electronegativity of the heteroatom, which is in the order NH > O > S > N-propyl. DFT data in Table 3 show that the NBO charges of N_1 decrease from **C1**-**C4**. The back donation of electron density towards the ligand from the metal centre due to the influence of the electronegativity of the heteroatom on the inert ligand shortens the Ru-N_1 bond length, thereby lengthening the Ru-Cl bond and thus enhancing reactivity as shown by the trend in the bond lengths (Table 3).

Higher rate of displacement of coordinated chloride in **C2** (O-atom) in comparison to **C3** (S-atom) is because oxygen is more electronegative than sulphur [44]. The DFT data show that the negative NBO charges of the heteroatoms decrease from **C1**-**C3**, leading to a decrease in the removal of electrons from the metal centre, making it more electrophilic and hence decreasing the rate of substitution reaction. This observation is in line with the observed second order rate constant, k_2, values. The high rate of substitution of the chlorides observed for **C1** (N-H) is associated with the presence of the acidic amine proton which is electron deficient

and hence withdraws electrons from the nitrogen atom enhancing its electron withdrawal ability; this then increases the π-back donation effect of the ligand, thereby increasing the electrophilicity of the metal centre and thus the reactivity.

The rate of displacement of coordinated chlorides in **C4** (N-propyl) by the nucleophiles decreased by a factor of about 10 compared to **C1**. Addition of the alkyl group (N-propyl in **C4**), which is an electron donor, reduces electron withdrawing ability of the nitrogen atom and consequently lowering π-back donation. This argument is supported by the DFT data that show that the positive NBO charges of the ruthenium(III) metal centre decrease from **C1**-**C4**. The DFT data shows that the N_1-Ru bond length follows the order **C1 < C2 < C3 < C4**, which is opposite to the Ru-Cl bond lengths that follow the order, **C1 > C3 > C2 > C4**. This observation affirms the argument that back donation of electron density from ruthenium(III) to the ligand shortens the N_1-Ru bond and lengthens the Ru-Cl bond.

DFT calculated frontier orbitals (Table 2) demonstrate that the electron density of the HOMO orbitals mostly lies on the ruthenium(III) metal centre and the chloride ligands while the LUMO electron density is largely located on the ligand framework, an indication of the influence from the metal centres due to their strong π-acceptor ability. This therefore creates a high electron density condition in both the occupied and unoccupied orbitals, and thus the ΔE(gap) decreases with the increase in the electronegativity of the atoms on the framework of the ligand. The observed comparable ΔE /eV of 3.12, 3.14, 3.16 and 3.83 for **C1, C2, C3** and **C4**, respectively.

In all of these studies a reverse reaction was not observed. Only a single step, considered to be the substitution of the coordinated chlorides was observed with no solvation pathway. Due to

the symmetrical nature of the mononuclear ruthenium(III) complexes, the three chloride ligands are equally susceptible to substitution which happens simultaneously. Comparing the rates of substitution by nucleophiles, TU, DMTU and TMTU these followed their steric hindrance ability with TMTU being the most sterically hindered nucleophile hence being the least reactive [45-46]. The observed relatively low $\Delta H^{\ddagger}$ and negative $\Delta S^{\ddagger}$ values is in line with the associative mode of activated process [47-48]. The negative $\Delta S^{\ddagger}$ values signifies a decrease in disorder due to the bond formation in the transition state [49-50].

A preliminary investigation of complexes **C1**-**C4** as potential anticancer drugs was carried out *in vitro* using HeLa cells (Table 4). The anti-cancer drug, doxorubicin, which was used as standard (reference drug), was potent in killing the cells, whereas the complexes had little cytotoxic effect. In anti-cancer drug discovery and design, inhibition of target biomolecules and selectivity of action are very essential. While current results have not established a potential for the tested complexes as anti-cancer agents, our future studies will examine the effects of the complexes on a wider panel of cancer cells and on normal cells, in order to understand whether there exist any differential cytotoxic sensitivities to the complexes of a variety of cells representing different cancers, consistent with the heterogeneous nature of the pathology and also with a number of reports suggesting that HeLa cells could be resistant to (pyridyl)benzoazole ligands and their respective ruthenium(III) complexes [52-54]. The inactivity of the complexes **C1**-**C4** could also be largely attributable to the low aromaticity (low number of the conjugated rings) of the (pridyl)benzoazole ligands, as found in a previous anti-cancer study of the ruthenium complexes [20], or to potential difficulty in their penetrating the cells to access and overwhelm target survival machineries to induce cell death. Poor cytotoxicity of the complexes could also be due to their relatively lower rate of substitution kinetics [17-20].

The docking experiments show the best possible intercalation between DNA groove structure and metal complexes. The most stable docked poses suggest that all investigated complexes interact in a parallel manner with respect to the minor groove of the DNA backbone (Table 5). The molecular docking results reveal that the investigated ruthenium(III) complexes approach the DNA site forming stable complexes through non-covalent interactions like hydrogen bonding and hydrophobic and van der Waals interactions. The relative binding energies of the complexes, summarised in Table 5, show the significant binding pattern of the complexes with the DNA [55]. The more negative the relative binding energy, the stronger the binding between DNA and complexes. Therefore, **C4** has a stronger binding ability compared to other complexes, which may be due to its electronic property that favours the stacking interactions between DNA base pairs leading to hydrogen bonding and van der Waals and hydrophobic interactions. It was observed that the binding energies are directly proportional to the kinetic stability of the investigated complexes (the most kinetically stable complex having the lowest second-order rate constant, k_2).

Conclusion

The study clearly demonstrated that the reactivity of ruthenium(III) complexes anchored on bidentate (pyridyl)benzoazole ligands can be systematically be tuned by varying the identity of the heteroatoms. The order of reactivity for the substitution of the chloride ligands by the thiourea ligands decreased in the order of **C1** > **C2** > **C3** > **C4** and this trend is due to electronic effect which iis linked to the electronegativity of the heteroatoms. This observation is supported by the DFT DATA. The displacement of the coordinated chlorides was also found to be sensitive towards the steric hindrance of the incoming nucleophiles. The observed $\Delta H^{\ddagger}$ and $\Delta S^{\ddagger}$ supported an associative mode of activation. The studied compounds exhibit poor cytotoxicity when compared to the reference compound, doxorubicin. The binding energies of the studied

complexes are inversely proportional to the rates of kinetic substitution. This study is of great importance for the development of new ruthenium anticancer drugs with reduced side effects.

References

[1] J. Yellol, S. A. Pérez, A. Buceta, G. Yellol, A. Donaire, P. Szumlas, P. J. Bednarski, G. Makhloufi, C. Janiak, A. Espinosa, J. Ruiz, J. Med. Chem. 58 (2015) 7310.

[2] J. Yellol, S. A. Pérez, G. Yellol, J. Zajac, A. Donaire, G. Vigueras, V. Novohradsky, C. Janiak, V. Brabec, J. Ruiz, J. Chem. Commun. 52 (2016) 14165.

[3] E. Wachter, A. Zamora, L. Nease, D. K. Heidary, J. Ruiz, E. C. Glazer, Chem. Comm. 52 (2016) 10121.

[4] A. Zamora, C. A. Denning, D.K, Heidary, E. Wachter, L. A. Nease, J. Ruiz, E. C. Glazer, Dalton Trans. 46 (2017) 2165.

[5] C. S Allardyce, P. J. Dyson, Platin. Met. Rev. 45 (2001) 62.

[6] G. Süss-Fink, Dalton Trans. 39 (2010) 1673.

[7] C. H. Leung, H. J. Zhong, D. D .H. Chan, D. L. Ma, Coord. Chem. Rev. 257 (2013) 1764.

[8] Adeniyi, A. A.; Ajibade, P. A. Rev Inorg Chem. 36 (2016) 53-75.

[9] L. Messori, P. Orioli, D. Vullo, E. Alessio, E. Iengo, The FEBS J. 267 (2000) 1206.

[10] E. Gallori, C. Vettori, E. Alessio, F. G. Vilchez, R. Vilaplana, P. Orioli, L. Messori, Arch. Biochem. Biophys, 376 (2000) 156.

[11] W. H. Ang, P. J. Dyson, Eur. J. Inorg. Chem. (2006) 4003.

[12] C. X. Zhang, S. J Lippard, Curr Opin Chem Biol. 7 (2003) 481.

[13] A. L. Noffke, A. Habtemariam, A. M. Pizarro, P.J. Sadler, Chem. Commun. 48 (2012) 5219.

[14] N. P. Barry, J. P. Sadler, Chem. Commun. 49 (2013) 5106.

[15] C. G. Hartinger, N. Metzler-Nolte, P. J. Dyson, Organometallics, 31 (2012) 5677.

[16] C. G. Hartinger, M. Groessl, S. M. Meier, A. Casini, P. J Dyson, Chem. Soc. Rev. 42 (2013) 6186.

[17] A. Rilak, I. Bratsos, E. Zangrando, J. Kljun, I. Turel, Ž. D. Bugarčić, E. Alessio, Inorg. Chem. 53 (2014) 6113.

[18] A. Rilak, R. Puchta, Ž. D. Bugarčić, Polyhedron, 91 (2015) 73.

[19] D. Lazić, A. Arsenijević, R. Puchta, Ž. D. Bugarčić, A. Rilak, Dalton Trans. 45 (2016) 4633.

[20] P. Čanović, A. R. Simović, S. Radisavljević, I. Bratsos, N. Demitri, M. Mitrović, Ž. D. Bugarčić, J. Biol. Inorg. Chem. 22 (2017) 1007.

[21] M. M. Milutinović, S. K. Elmroth, G. Davidović, A. Rilak, O. R. Klisurić, I. Bratsos, Ž. D. Bugarčić, Dalton Trans. 46 (2017) 2360.

[22] E. Alessio, G. Mestroni, A. Bergamo, G. Sava, G. Curr. Top. Med. Chem. 4 (2004) 1525.

[23] M. Bacac, A.C. Hotze, K. van der Schilden, J.G. Haasnoot, S. Pacor, E. Alessio, J. Reedijk, J. Inorg. Biochem. 98 (2004) 402.

[24] L. Giovagnini, S. Sitran, I. Castagliuolo, P. Brun, M. Corsini, P. Zanello, D. Fregona, Dalton Trans. 47 (2008) 6699.

[25] S. Scintilla, L. Brustolin, A. Gambalunga, F. Chiara, A. Trevisan, C. Nardon, D. Fregona, J. Inorg. Biochem. 166 (2016) 76.

[26] C. Nardon, L. Brustolin, D. Fregona, Future Med. Chem. 8 (2016) 211.

[27] N. Park, Y. Heo, M. R. Kumar, Y. Kim, K. H. Song, S. Lee, Eur. J. Org. Chem. 10 (2012) 1984.

[28] A.O Ogweno, S.O. Ojwach, M. P. Akerman, Dalton Trans. 43 (2014) 1228

[29] A. Mambanda, D. Jaganyi, Dalton Trans. 40 (2011) 79.

[30] G.W. Trucks, M.J. Frisch, H.B. Schlegel, G.E. Scuseria, J.R. Cheeseman, M.A. Robb, G. Scalmani, V. Barone, G.A. Petersson, B. Mennucci, H. Nakatsuji, M. Caricato, X. Li, A.F. Izmaylov, H.P. Hratchian, J. Bloino, G. Zheng, M. Hada, J.L. Sonnenberg, M. Ehara, K. Toyota, R. Fukuda, M. Ishida, J. Hasegawa, T. Nakajima, Y. Honda, O. Kitao, T. Vreven, H. Nakai, J.A. Montgomery Jr, J.E. Peralta, M. Bearpark, F. Ogliaro, J.J. Heyd, E. Brothers, K.N. Kudin, R. Kobayashi, V.N. Staroverov, J. Normand, K. Raghavachari, J.C.B.A Rendell, S.S. Iyengar, J. Tomasi, M. J.M.M.N. Cossi, M. Rega, Klene, J.E. Knox, J.B. Cross, C. Adamo, V. Bakken, J. Jaramillo, R. Gomperts, R.E. Stratmann, O. Yazyev, A.J. Austin, R. Cammi, C. Pomelli, R.L. Martin, J.W. Ochterski, K. Morokuma, V.J. Zakrzewski, G.A. Voth, P. Salvador, J.J. Dannenberg, S. Dapprich, O. Farkas, A.D. Daniels, J.B. Foresman, J.V. Ortiz, J. Cioslowski, D.J. Fox, Gaussian 09 (RevisionA. 1), Inc., Wallingford, CT (2009)

[31] A. D. Becke, Phys. Rev. Applied. 38 (1988) 3098.

[32] S. Grimme, J. Comput. Chem. 25 (2004) 1463.

[33] M. Cossi, N. Rega, G. Scalmani, V. J. Barone, Comput. Chem. 24 (2003) 669.

[34] Z. Chval, M. Sip, J. V. Burda, J. Comp. Chem. 29 (2008) 2370.

[35] B. J. Taiwo, A. A. Fatokun, O. O. Olubiyi, O. T. Bamigboye-Taiwo, F. R. van Heerden, C. W. Wright, Bioorganic Med. Chem. 25 (2017) 2327.

[36] M. Altaf, M. Monim-ul-Mehboob, A. A. Isab, V. Dhuna, G. Bhatia, K. Dhuna, S. Altuwaijri, New J. Chem. 39 (2015) 377.

[37] ACD/ChemSketch, Advanced Chemistry Development, Inc., Toronto, ON, Canada, 2015. www.acdlabs.com.

[38] C. F. Macrae, I. J. Bruno, J. A. Chisholm, P. R. Edgington, P. McCabe, E. Pidcock, L. Rodriguez-Monge, R. Taylor, J. van de Streek, P. A. Wood, J. Appl. Cryst. 41 (2008) 466.

[39] H. R. Drew, R. M. Wing, T. Takano, C. Broka, S. Tanaka, K. Itakura, R. E. Dickerson, Proc. Natl. Acad. Sci. U. S. A. 78 (1981) 2179.

[40] E. F. Pettersen, T. D. Goddard, C. C. Huang, G. S. Couch, D. M. Greenblatt, E. C. Meng, T. E. Ferrin, J. Comput. Chem, 25 (2004) 1605.

[41] Origin7.5TM SRO, v7.5714 (B5714); Origin Lab Corporation: Northampton, OH, 2003.

[42] J. D. Atwood, Inorganic and Organometalic Reaction Mechanisms,Whiley-*VCH* Inc., NY; 2nd ed., 1997.

[43] D. Das, S. S. Mohapatra, S. Roy, Chem. Soc. Rev. 44 (2015) 3666.

[44] W. Gordy, W. O. Thomas, J. Chem. Phys. 24 (1956) 439.

[45] P. O. Ongoma, D. Jaganyi, Dalton Trans. 42 (2013) 2724.

[46] D. Jaganyi, D. Reddy, J. A. Gertenbach, A. Hofmann, R. van Eldik, Dalton Trans. (2004) 299.

[47] A. Mambanda, D. Jaganyi, Dalton Trans. 41 (2012) 908.

[48] D. Jaganyi, A. Mambanda, S. Hochreuther, R. van Eldik, Dalton Trans. 39 (2010) 3595.

[49] D. Jaganyi, K. L. De Boer, J. Gertenbach, J. Perils, Int. J. Chem. Kinet. 40 (2008) 808.

[50] F. Basolo, R. G. Pearson, Mechanisms in Inorganic Reactions, 2nd Ed., Wiley, New York, 1967.

[51] G. Matlashewski, L. Banks, D. Pim, L. Crawford, Eur. J. Biochem. 154 (1986) 665.

[52] M. Scheffner, B. A. Werness, J. M. Huibregtse, A. J. Levine, P. M. Howley, Cell, 63 (1990) 1129.

[53] E. Ramachandran, P. Kalaivani, R. Prabhakaran, M. Zeller, J. H. Bartlett, P. O. Adero, T. R. Wagner, K. Natarajan, Inorg. Chim. Acta. 385 (2012) 94.

[54] D. Das, A. Dutta, P. Mondal, RSC Adv. 4 (2014) 60548.